LANGMUIR

pubs.acs.org/Langmuir Article

How Do Amphiphilic Biopolymers Gel Blood? An Investigation Using Optical Microscopy

Ian C. MacIntire, Matthew B. Dowling,* and Srinivasa R. Raghavan*

Cite This: *Langmuir* 2020, 36, 8357−8366 Read Online

ACCESS | Metrics & More | Article Recommendations | Supporting Information

ABSTRACT: Amphiphilic biopolymers such as hydrophobically modified chitosan (hmC) have been shown to convert liquid blood into elastic gels. This interesting property could make hmC useful as a hemostatic agent in treating severe bleeding. The mechanism for blood gelling by hmC is believed to involve polymer−cell self-assembly, i.e., insertion of hydrophobic side chains from the polymer into the lipid bilayers of blood cells, thereby creating a network of cells bridged by hmC. Here, we probe the above mechanism by studying dilute mixtures of blood cells and hmC in situ using optical microscopy. Our results show that the presence of hydrophobic side chains on hmC induces significant clustering of blood cells. The extent of clustering is quantified from the images in terms of the area occupied by the 10 largest clusters. Clustering increases as the fraction of hydrophobic side chains increases; conversely, clustering is negligible in the case of the parent chitosan that lacks hydrophobes. Moreover, the longer the hydrophobic side chains, the greater the clustering (i.e., $C_{12} > C_{10} > C_8 > C_6$). Clustering is negligible at low hmC concentrations but becomes substantial above a certain threshold. Finally, clustering due to hmC can be reversed by adding the supramolecule α-cyclodextrin, which is known to capture hydrophobes in its binding pocket. Overall, the results from this work are broadly consistent with the earlier mechanism, albeit with a few modifications.

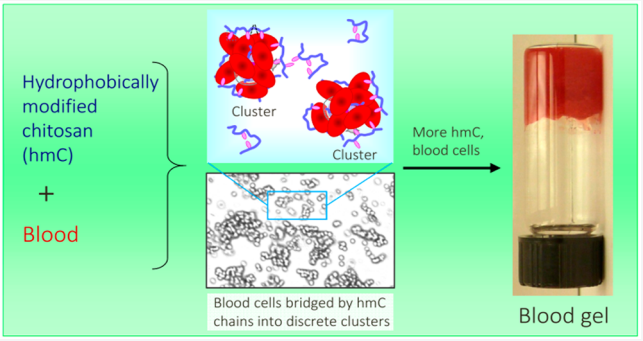

INTRODUCTION

The self-assembly of amphiphilic polymers in water continues to be a topic of great scientific interest.[1,2] Water-soluble amphiphilic polymers typically have a hydrophilic backbone and hydrophobic tails tethered to the backbone. As a specific example, if the backbone is the cationic polysaccharide chitosan, it is converted into an amphiphilic polymer by attaching *n*-alkyl tails to some of the amines along the backbone (Figure 1).[3−5] The resulting polymer, termed hydrophobically modified chitosan (hmC), is still soluble in water, provided the tails are not too long and there are only a few tails per chain. The hydrophobic tails on adjacent hmC chains will then associate via hydrophobic interactions, both with each other as well as with other colloidal species in the water.

Over the past 15 years, our lab has studied hmC in conjunction with various structures covered by lipid membranes, including vesicles[6−8] and biological cells.[9,10] First, we showed that when hmC was added to nanoscale vesicles, the flowing liquid was converted into an elastic gel. Thereafter, we demonstrated similar gelation when hmC was mixed with liquid blood (either human or bovine). Gelation was confirmed by rheological techniques and could be demonstrated visually by the "vial inversion test", i.e., the ability of gel samples to hold their weight in the overturned vial (Figure 1b). Importantly, while gelation occurred with hmC, it did not occur with the parent polymer (chitosan) (Figure 1a),[9,10] showing that hydrophobes were essential for gelation. Also, in our experiments, heparin or sodium citrate was added to the blood to prevent its coagulation via the blood-clotting cascade; thus, gelation by hmC was unrelated to clotting. Moreover, gelation did not ensue when hmC was added to the cell-free (protein) component of blood, i.e., blood plasma.[9] Thus, gelation by hmC was unrelated to biochemical mechanisms but simply required the presence of blood cells. Moreover, hmC also gelled other kinds of biological cells including mammalian endothelial cells.[10]

The mechanism for the gelation of microscale blood cells (as well as nanoscale vesicles) by hmC has been hypothesized to involve hydrophobic interactions.[6−10] Specifically, some of the hydrophobic tails on hmC are expected to embed in the lipid membranes of blood cells (the interiors of these bilayer membranes are hydrophobic due to the lipid tails being located there[11−13]). Through such hydrophobic anchoring, each hmC

Received: February 12, 2020
Revised: June 9, 2020
Published: July 17, 2020

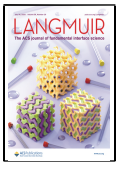

https://dx.doi.org/10.1021/acs.langmuir.0c00409
Langmuir 2020, 36, 8357−8366

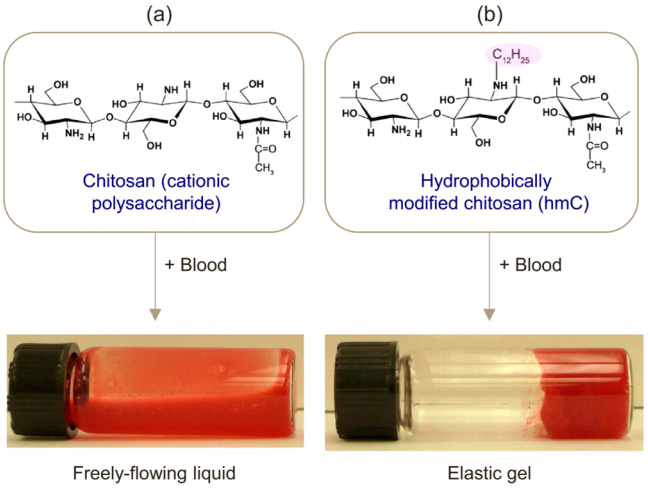

Figure 1. Effect of adding chitosan or hydrophobically modified chitosan (hmC) to blood. Here, bovine blood pretreated with sodium citrate (to prevent clotting) is used without dilution. Polymer concentration in both cases is 0.25 wt %. (a) Blood remains a flowable liquid when the parent chitosan (see structure) is added. (b) Adding hmC (obtained by attaching 5 mol % of C_{12} hydrophobes to the chitosan; see structure) converts the blood into a gel. The gel has a significant yield stress, which is why it is able to retain its weight in the overturned vial.

chain is expected to bind to multiple cells, i.e., the chains will *bridge* adjacent cells. Such bridging will result in a sample-spanning three-dimensional (3-D) network of cells connected by polymer chains,[9,10] which can explain the gelation of the blood samples.

Support for the above mechanism comes from various related experiments. For example, other amphiphilic polymers, including hydrophobically modified variants of alginate (hmA),[10] poly(ethylene oxide) (hm-PEO),[14−16] hydroxyethyl-cellulose (hm-HEC),[12,17] and hyaluronic acid (hm-HYA),[18] have also been shown to form gels when mixed either with blood, with other cells, or with vesicles. Others have used hmC to form gels in conjunction with various cells, including bacteria.[19−22] Moreover, our lab has further established that gelation of blood[9,10] (or vesicles[8]) by hmC can be reversed by adding α-cyclodextrin (α-CD), which is a barrel-shaped supramolecule with a hydrophobic binding pocket. Such "ungelling" is hypothesized to occur because α-CD molecules can sequester the hydrophobes on hmC within their binding pockets, thereby preventing the chains from connecting adjacent cells.[8−10] Thus, the very fact that α-CD works as an ungelling agent points to hydrophobic interactions as being responsible for gelation in the first place.

The gelling of blood by hmC is not just of academic interest. This property suggests that hmC could serve as a "**hemostatic agent**"[23] and stop bleeding from wounds. Uncontrolled hemorrhage from traumatic injury is a leading cause of death for people aged 46 and under.[9,23] This includes both civilian victims of accidents or violent altercations as well as soldiers in the theater of war. To test the hemostatic ability of hmC, we conducted studies with animal models in collaboration with trauma surgeons. We found that hmC-based solid dressings could arrest bleeding from even the most severe injuries (such as a puncture of the femoral artery in pigs), whereas a corresponding dressing made with native chitosan was unable to contain the same.[9,24] In addition, hmC-based gels and foams and hmC-coated gauze have all been shown to act as effective hemostatic agents in various injury models.[24−26] Thus, hmC offers significant potential as a hemostatic agent.

The practical utility of hmC as a hemostatic agent underscores the need to better understand the mechanism by which it gels blood. While the postulated mechanism is reasonable, the evidence for it has been mostly indirect.[9,10] *In this study, we attempt to substantiate this mechanism by directly probing the microstructure in hmC−blood mixtures.* Since blood cells are microscale structures, they can be directly visualized by optical microscopy. We therefore set out to study mixtures of blood cells and hmC using bright-field optical microscopy. Results for hmC are compared with those for the parent chitosan. Important variables in our study include the degree of hydrophobic modification, the polymer molecular weight, and the polymer concentration. In addition, we also study hmC−blood mixtures after addition of various cyclodextrins to probe the ability of the latter to ungel the mixtures. Overall, the results from this work support the earlier mechanism, but they do suggest a few important modifications.

EXPERIMENTAL SECTION

Materials. Chitosan was purchased from Primex (Iceland), and it had a nominal molecular weight of 250 000. This was used in most cases as the parent polymer to synthesize the hmC. A second chitosan with a molecular weight of 100 000 was also purchased from Primex for comparison purposes. Both polymers were 99% deacetylated. Sodium cyanoborohydride and the alkyl aldehydes with *n*-dodecyl (C_{12}), *n*-decyl (C_{10}), *n*-octyl (C_8), and *n*-hexyl (C_6) chains were obtained from Sigma-Aldrich. Alpha-cyclodextrin (α-CD), methyl-beta-cyclodextrin (mβ-CD), and hydroxypropyl-beta-cyclodextrin (hpβ-CD) were obtained from TCI America. Citrated bovine whole blood was purchased from Lampire Biological Laboratories. Mouse fibroblast L929 cells were obtained from ATCC, as were reagents for cell culture, including Eagle's MEM culture media, fetal bovine serum (FBS), penicillin, and streptomycin.

Synthesis. hmC was synthesized using the procedure described previously.[3,6] Briefly, chitosan was dissolved at 1% w/v in a 0.2 M acetic acid solution. An equal volume of ethanol was then added as a cosolvent before the temperature was increased to 55 °C. Varying amounts of *n*-alkyl aldehyde were dissolved in ethanol and mixed into the chitosan solution to give varying levels of hydrophobic modification (0.5, 1.0, 2.0, and 5.0 mol % relative to the amines on chitosan chains). The reaction mixture was treated with an aqueous solution of sodium cyanoborohydride and left to react overnight. Afterward, the hmC was precipitated by raising the pH to around 10. The precipitate was purified by multiple washes of ethanol and water and then dried to a powder.

Solution Preparation. hmC was dissolved in 0.04 M acetic acid solution at various concentrations. Sodium chloride was then added at a concentration of 0.9% w/v for osmotic balance. The bovine blood was diluted (10×) with normal saline. The pH of the blood was ∼7, while the pH of the hmC solutions was ∼3. The cell concentration in the blood is expected to be $\sim 10^8$ cells/mL.

Cell Culture. ATCC L929 mouse fibroblasts were cultured in Eagle's MEM media supplemented with 5% FBS, 50 IU/mL penicillin, and 0.05 mg/mL streptomycin. Cells were harvested, pelleted by centrifugation, and resuspended to give a cell concentration of approximately 2×10^7 cells/mL in normal saline.

Optical Microscopy. To prepare a sample for microscopic observation, 20 μL of the hmC solution was pipetted onto a glass slide. A 20 μL amount of diluted blood (or L929 cell suspension) was then added. The combined solutions were mechanically mixed with a stirring rod, and a coverslip was placed on top of the sample. Samples were then imaged immediately using an Olympus IX51 microscope at 100× and 400× magnification. A Hamamatsu A3472-06 camera was used to capture multiple micrographs for each sample.

https://dx.doi.org/10.1021/acs.langmuir.0c00409
Langmuir 2020, 36, 8357−8366

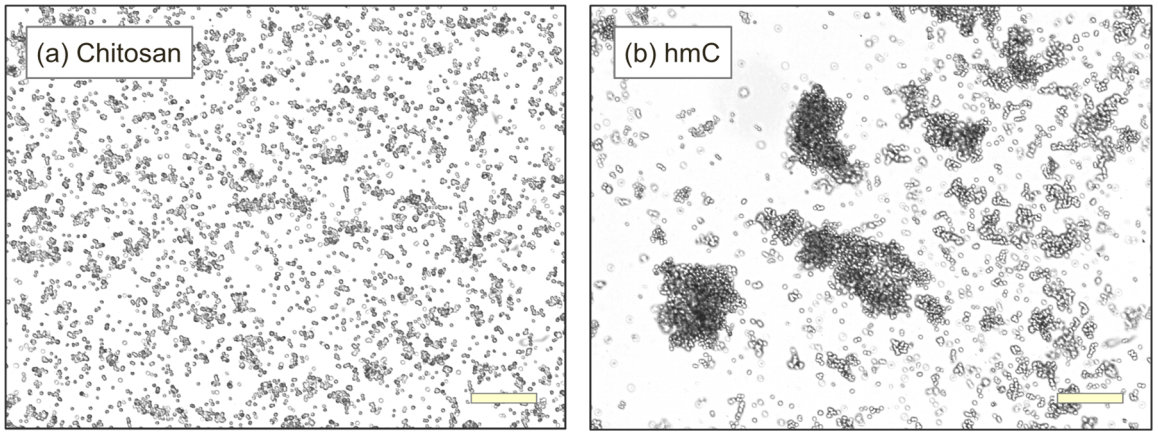

Figure 2. Effect of adding chitosan or hmC to blood. Citrated bovine blood is diluted 10× relative to that used in Figure 1. This blood is mixed with 0.05 wt % of (a) chitosan and (b) hmC (having 5 mol % of C_{12} hydrophobes). Images of the samples from optical microscopy are shown. Note the significant clustering of blood cells in b compared to a. Scale bars are 100 μm.

Image Analysis. Clustering in the samples was analyzed using the ImageJ program. Images were thresholded and subjected to the ImageJ particle analyzer function. The sizes of all clusters greater than 48 μm^2 were recorded for each sample. For a given sample, several parameters were calculated to obtain an estimate for the extent of clustering. The measure used here, as described below, is the fraction of the image area occupied by the 10 largest clusters.

RESULTS

We performed our experiments with bovine blood. As with human blood, it is a combination of different cell types (red cells, white cells, platelets), but the red blood cells (RBCs) are by far the most abundant, and these typically have diameters of about 6−8 μm.[27] The blood used here has been treated with sodium citrate, which is a known inhibitor of the blood-clotting cascade.[28] Elimination of any interference from the clotting cascade is important for our experiments. Another inhibitor of blood clotting is the biopolymer, heparin.[28] As demonstrated previously,[9,10] hmC can gel both citrated as well as heparinized blood, which shows that this gelation is independent of the clotting cascade. Here, we chose to use citrated blood for all of our experiments. One reason to avoid heparin is that it is an anionic macromolecule that can interact electrostatically with the cationic chitosan and hmC. Thus, by using citrated blood, we avoid complications due to electrostatic effects, which makes our results easier to interpret.

The protocol for our microscopic studies involves combining 20 μL of polymer (hmC or chitosan) solution with 20 μL of citrated blood on a microscope slide, quickly mixing the two on the slide, and observing the mixture thereafter by bright-field microscopy. In the polymer solution, we included 0.9% w/v of NaCl for osmotic balance with blood cells. This was important to ensure that the blood cells did not suffer osmotic stress when mixed with the polymer solution. With regard to the blood, we diluted the original stock solution by 10× in normal saline. This was done because at the original concentration the density of blood cells was too high when viewed under the microscope, which made it difficult to distinguish if the cells were lying on top of each other or undergoing aggregation. With the diluted blood (cell concentration $\approx 10^8$ cells/mL), the cells could be resolved better, as shown below.

Figure 2 shows representative images at 100× magnification of a mixture of the above blood with 0.05 wt % of hmC or the parent chitosan. The hmC in these experiments was obtained by modifying a chitosan of 250 kDa molecular weight with C_{12} hydrophobes with the degree of modification being 5 mol % with respect to the amines on the chitosan. Note that the cells seen in the image are all RBCs. The two images in the figure illustrate the key differences between the two polymers. When chitosan is added (Figure 2a), the blood cells remain as mostly discrete structures. (This image is virtually identical to those of the blood cells without adding any polymer.) There may be at most a few small clusters of cells, although it is not clear if these are truly clusters or if the cells are simply overlapping (but unconnected) at the same spot in the image. In comparison, when hmC is added, the majority of blood cells are clustered (Figure 2b). The clusters in this case are dense structures and consequently appear dark in the image. Because most of the cells are in clusters, there is considerable "empty" space in the image where no cells are seen. Thus, we infer that hmC induces blood cells to cluster, while chitosan does not. A closer look at the clusters induced by hmC are shown in the two images of Figure 3. These again reveal the clusters to be dense aggregates of individual cells. All of the cells appear to be intact, and there is no obvious disruption or hemolysis of the cells.

Similar results were also obtained with cells other than blood. Specifically, we studied L929 mouse fibroblast cells (∼10−20 μm in size), which were resuspended in normal saline at a concentration of about 2×10^7 cells/mL. This cell suspension was combined with 0.05 wt % of hmC (with 5 mol % C_{12} hydrophobes) or chitosan, and representative images are shown in Figure 4. We again observe that the cells remain as discrete structures when combined with chitosan (Figure 4a). However, when combined with the hmC (which is the same as above), the cells become aggregated into large and dense clusters (Figure 4b).

We then attempted to *quantify* the differences between images of clustered and unclustered cells, such as those in Figure 2a vs 2b or Figure 4a vs 4b. We used the ImageJ software to analyze the images. The software can threshold the image and identify the outlines of all "clusters" (defined as those with a size > 48 μm^2, which is the approximate area of a single RBC)[27] and thereby also make a cluster size distribution. This is shown by Figures S1 and S2 in the Supporting Information. However, as noted above, it is not clear in the case of the chitosan samples (Figures 2a and 4a) if there are

https://dx.doi.org/10.1021/acs.langmuir.0c00409
Langmuir 2020, 36, 8357−8366

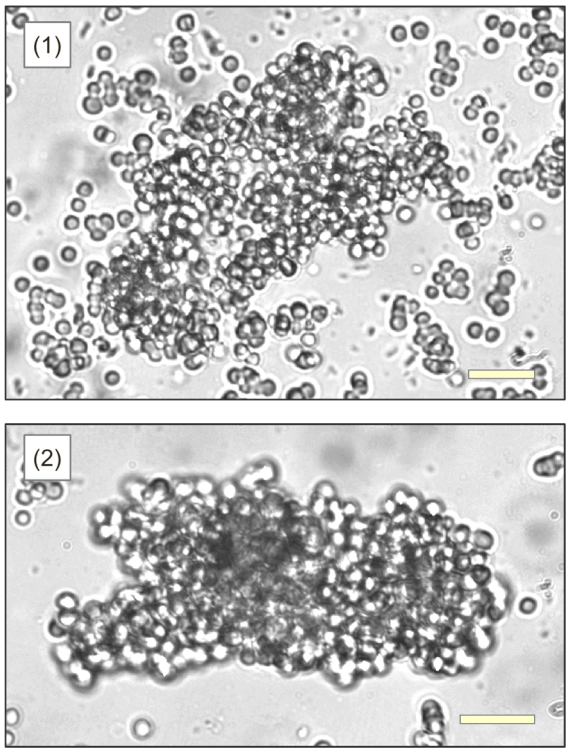

Figure 3. Close ups of blood-cell clusters induced by hmC. These are from Figure 2b, i.e., for mixtures of citrated bovine blood with 0.05 wt % hmC (C_{12}, 5 mol %). Scale bars are 20 μm.

indeed clusters or if the cells are merely overlapping. For this reason, measures such as the fraction of cells in clusters or the average sizes of clusters were not reliable ways to differentiate between samples (Figure S2). Note that the key information is contained in the largest clusters, which are a very small fraction of the distribution in terms of number density.

The procedure we chose to use is depicted in Figure S1. First, we threshold the image and identify the 10 largest clusters using ImageJ. The 10 largest clusters in Figure 2a and 2b (in decreasing order of size) are numbered in panels A and B of Figure S1. Next, we show the same fields of view in panels C and D after these "top 10" clusters are removed. Note that panel D looks very different from panel B because the "top 10" clusters in the hmC sample occupied a large fraction of the area. On the other hand, panels C and A look about the same because the "top 10" clusters in the chitosan sample were a small fraction of the area. This shows that the total area of the 10 largest clusters is one measure for quantifying the extent of clustering. We normalize this area by the total area occupied by all of the cells/clusters in the image. The same procedure is then repeated for 3 or more images from the same sample. The average and standard deviation are thus calculated for the normalized areal fraction (%) of the 10 largest clusters, which we term $A_{cluster}$. For the images in Figure 2, we calculate $A_{cluster}$ to be 5 $\pm$ 3% for the case of blood + chitosan (Figure 2a), whereas it is substantially higher at 62 $\pm$ 2% for blood + hmC (Figure 2b).

Using the above measure, we can quantify the effects of different variables on blood-cell clustering. First is the degree of hydrophobe modification, with the hydrophobe length maintained at C_{12}. We compared hmC variants with different degrees of C_{12} hydrophobes (0.5, 1, 2, and 5 mol % relative to the amine groups). Each of these was mixed with blood at a polymer concentration of 0.05 wt %. Figure 5A–D shows a systematic trend in the images, with the extent of blood-cell clustering increasing with the mol % of hydrophobes. These images were quantified by the procedure described in Figure S1, and the results for the cluster areal fraction ($A_{cluster}$) are presented in the bar graph in Figure 5E. An increase in $A_{cluster}$ with mol % hydrophobes is shown by the data, i.e., the more hydrophobes per chain, the more clustering.

Next, we tested *n*-alkyl hydrophobes of different lengths (C_6, C_8, C_{10}, C_{12}). Different variants of hmC with each of these hydrophobes were synthesized, with the degree of modification kept constant at 5 mol % relative to the amine groups. The different polymers were tested with blood at a polymer concentration of 0.05 wt %. Images for the different cases are shown in Figure 6A–D, and here, again the images show a systematic trend, i.e., that clustering increases with the length of the hydrophobes ($C_{12} > C_{10} > C_8 > C_6$). From these images, the cluster areal fractions ($A_{cluster}$) were extracted, and the results in Figure 6E show a steady increase in this parameter with increasing hydrophobe length.

We then studied different concentrations of the hmC that had 5 mol % of C_{12} hydrophobes. Images with blood for polymer concentrations spanning 4 orders of magnitude are shown in Figure 7A–D. No clustering of blood cells is seen at the lowest hmC concentration of 0.00005 wt % (Figure 7A). In

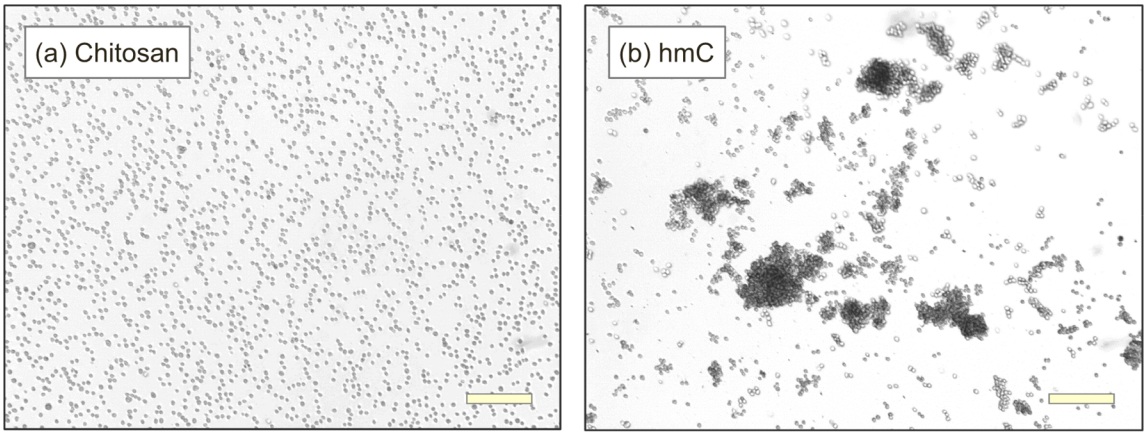

Figure 4. Effect of adding chitosan or hmC to L929 mouse fibroblast cells. Cells are combined with 0.05 wt % of (a) chitosan and (b) hmC (C_{12} hydrophobes, 5 mol %) and observed by optical microscopy. Note the significant clustering of cells in b compared to a. Scale bars are 400 μm.

https://dx.doi.org/10.1021/acs.langmuir.0c00409
Langmuir 2020, 36, 8357–8366

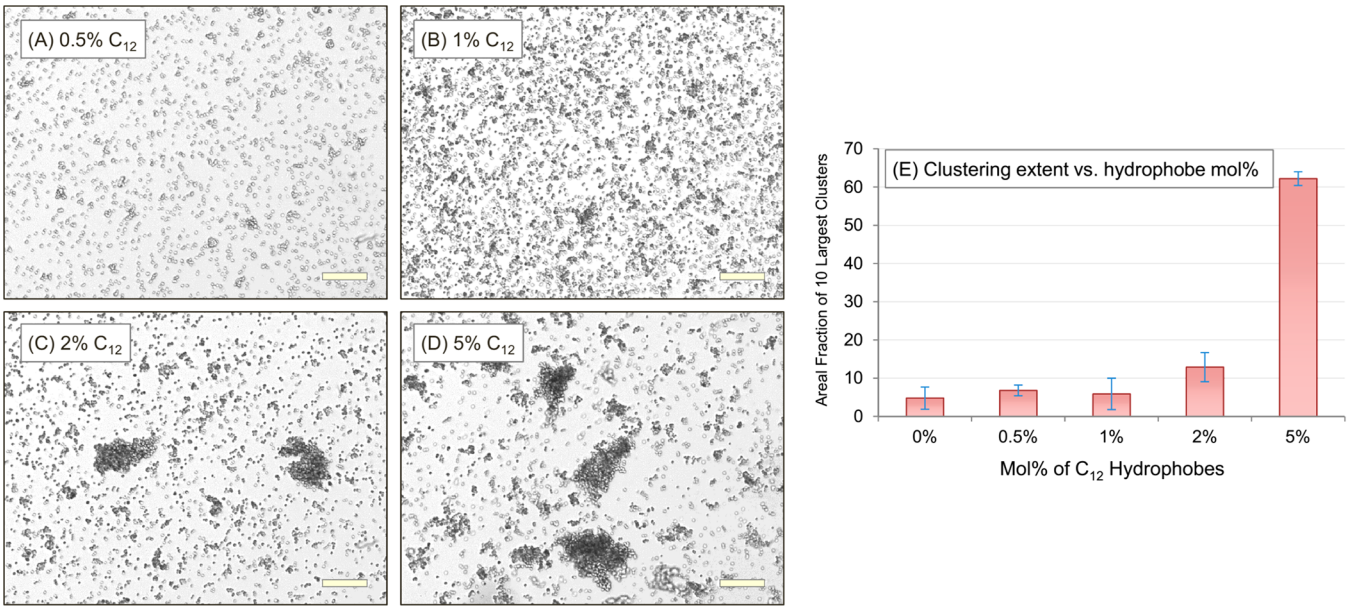

Figure 5. Effect of varying the degree of modification of hmC by C_{12} hydrophobes. Images are for citrated bovine blood mixed with 0.05 wt % of hmC having different mole percents of C_{12} hydrophobes: (A) 0.5%, (B) 1%, (C) 2%, and (D) 5%. Scale bars are 100 μm. (E) By analyzing the images, the extent of clustering is quantified (in terms of $A_{cluster}$, the areal fraction of the 10 largest clusters) and plotted against the hydrophobe mole percent. Error bars represent standard deviations from multiple measurements.

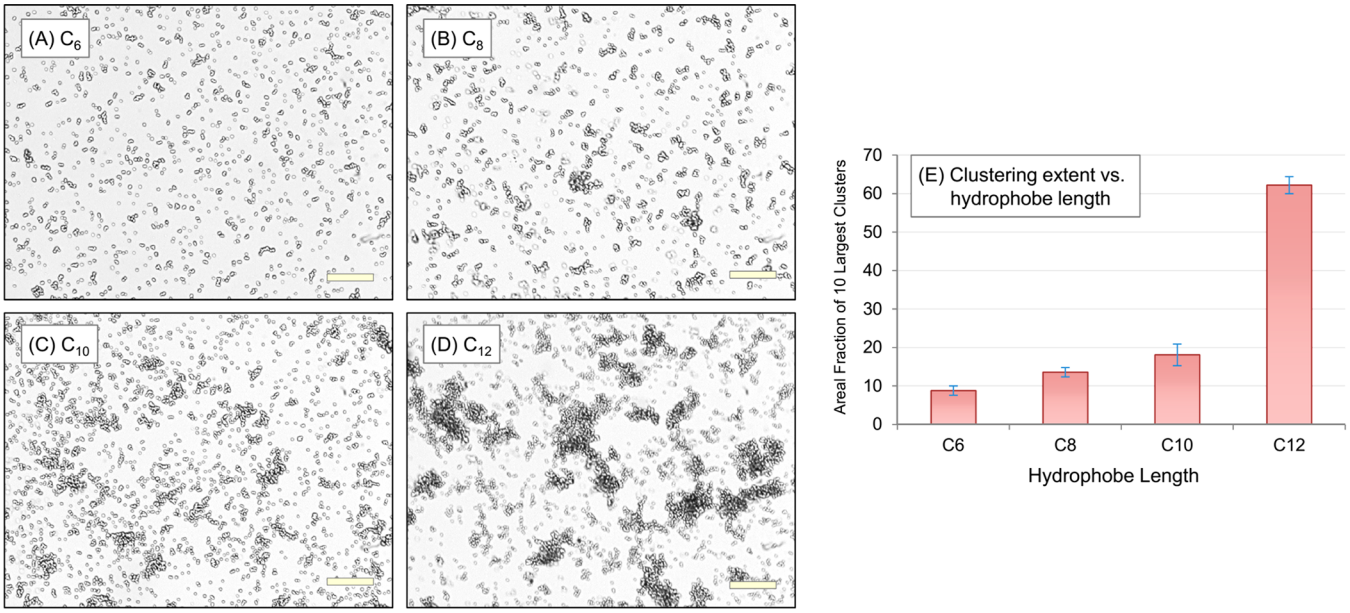

Figure 6. Effect of varying the length of hydrophobes on hmC. Images are for citrated bovine blood combined with 0.05 wt % of hmC containing different lengths of *n*-alkyl hydrophobes (5 mol % modification): (A) C_6, (B) C_8, (C) C_{10}, and (D) C_{12}. Scale bars are 100 μm. (E) By analyzing the images, the extent of clustering is quantified (in terms of $A_{cluster}$, the areal fraction of the 10 largest clusters) and plotted against the hydrophobe length. Error bars represent standard deviations from multiple measurements.

terms of number densities, this concentration translates to $\sim 10^{12}$ chains/mL, and we calculate that each chain has about 80 hydrophobes (based on the graft density). Thus, there are $\sim 10^{14}$ hydrophobes on the hmC chains, but this is insufficient to cause clustering of the $\sim 10^{8}$ blood cells/mL. However, significant clustering is observed when the hmC concentration is increased 10-fold to 0.0005 wt %, i.e., to $\sim 10^{13}$ chains/mL (Figure 7B). The cluster areal fractions ($A_{cluster}$) from these images are plotted in Figure 7E, and from the data, the clustering is nearly zero up to 0.00005 wt % and then remains practically the same for concentrations from 0.0005 to 0.05 wt % (i.e., spanning 2 orders of magnitude). Thus, for a polymer like the hmC tested here (with a large number of long hydrophobes), there appears to be a low threshold concentration beyond which clustering becomes significant.

The molecular weight (MW) of the hmC was also tested as an additional parameter. The polymers studied thus far had a molecular weight of 250 kDa. For comparison, we obtained a chitosan with a lower MW of 100 kDa and converted this to an hmC by attaching 5 mol % of C_{12} hydrophobes. The two polymers were combined with blood at a concentration of 0.05 wt %, and the corresponding images are shown in Figure 8.

https://dx.doi.org/10.1021/acs.langmuir.0c00409
Langmuir 2020, 36, 8357−8366

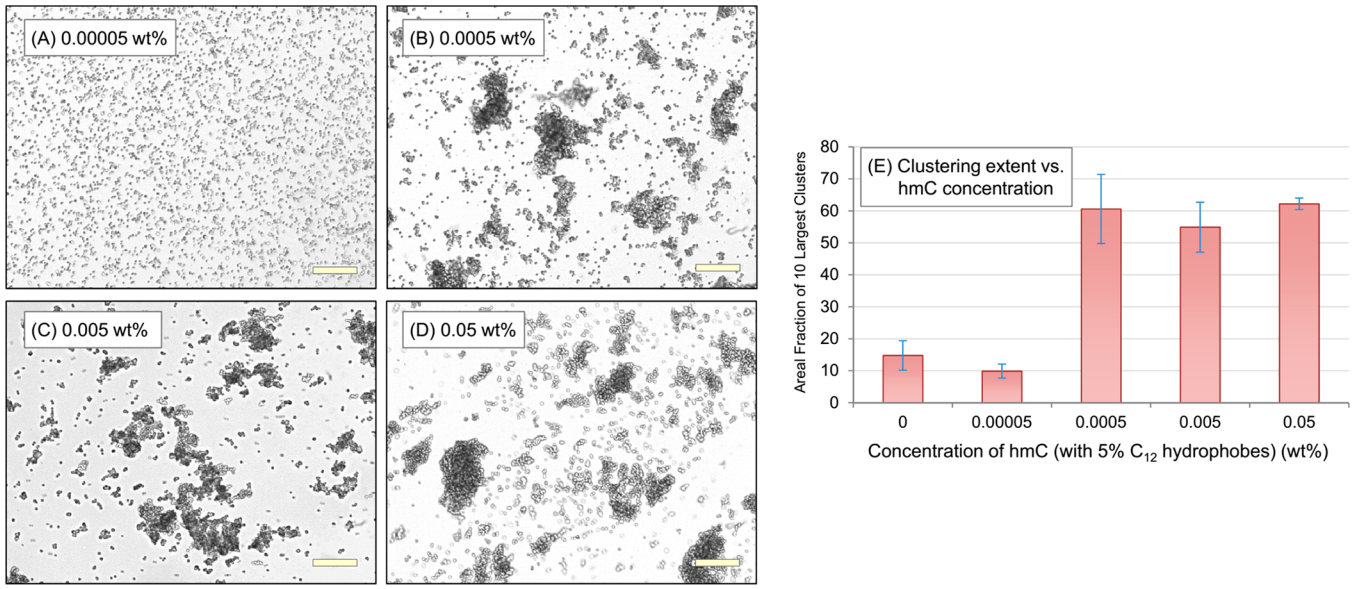

Figure 7. Effect of hmC concentration. Images are for citrated bovine blood combined with hmC (C_{12}, 5 mol %) at different concentrations: (A) 0.00005, (B) 0.0005, (C) 0.005, and (D) 0.05 wt %. Scale bars are 100 μm. (E) By analyzing the images, the extent of clustering is quantified (in terms of $A_{cluster}$, the areal fraction of the 10 largest clusters) and plotted against the hmC concentration. Error bars represent standard deviations from multiple measurements.

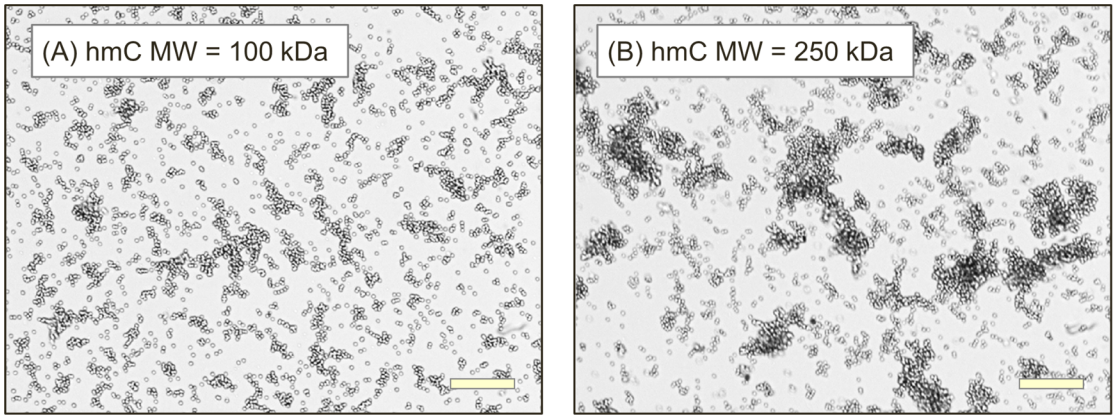

Figure 8. Effect of hmC molecular weight. Images are for citrated bovine blood combined with 0.05 wt % of hmC (C_{12}, 5 mol %) at two different molecular weights: (A) 100 and (B) 250 kDa. Scale bars are 100 μm.

The clustering in the case of the 100 kDa hmC (Figure 8A) is lower than that in the case of the 250 kDa polymer (Figure 8B). The cluster areal fraction ($A_{cluster}$) in the former case is 22 ± 3% compared to 62 ± 2% for the latter.

Finally, we examined whether clustering of blood cells could be reversed by adding cyclodextrins (CDs). In past studies,[8−10] the type of CD that was shown to reverse gelation of blood (or vesicles) was α-CD, and this was the one we first tested. Our first experiment involved mixing 20 μL each of blood and 0.05 wt % hmC solution on the microscope slide (causing cells to cluster) and thereafter adding 20 μL of 50 mM α-CD solution. The hmC is the one with 5 mol % of C_{12} hydrophobes. As a control, we substituted the α-CD solution with saline, and the result for this case (corresponding to blood +0.033 wt % hmC) is shown in Figure 9A. As expected, we see significant clustering. Next, Figure 9B shows an image of the above sample with added α-CD (concentration of 16.7 mM in the final mixture). In this case, the α-CD substantially reduces (but does not eliminate) the clustering: the cluster areal fraction ($A_{cluster}$) decreases from 45 ± 2% to 10 ± 4%. Interestingly, the order of addition makes a difference. We repeated the above experiment by first premixing the hmC solution with the α-CD and then adding this combination to blood (the final sample has the same concentrations of hmC and α-CD as above). In this case (Figure 9C), the clustering is almost eliminated, with $A_{cluster}$ dropping to 5 ± 1%.

We also compared other types of CDs for their ability to reduce or eliminate blood-cell clustering. In comparison to α-CD, which is based on a six-membered glucose ring and has a hydrophobic cavity of 0.57 nm, β-CD is based on a seven-membered glucose ring and thus has a larger hydrophobic cavity of 0.78 nm.[29] Due to this larger cavity, single-tailed *n*-alkyl hydrophobes fit poorly when inserted into the cavity of β-CD compared to α-CD, and thus, the binding interaction is weaker in the case of β-CD. Results for two derivatives of β-CD, i.e., mβ-CD and hpβ-CD, are shown in Figure S3. These two β-CD derivatives have higher solubility in water than the parent compound and are therefore extensively used in pharmaceutical formulations.[29] For our experiments, the same conditions as in Figure 9C were chosen, i.e., the CD

https://dx.doi.org/10.1021/acs.langmuir.0c00409
Langmuir 2020, 36, 8357−8366

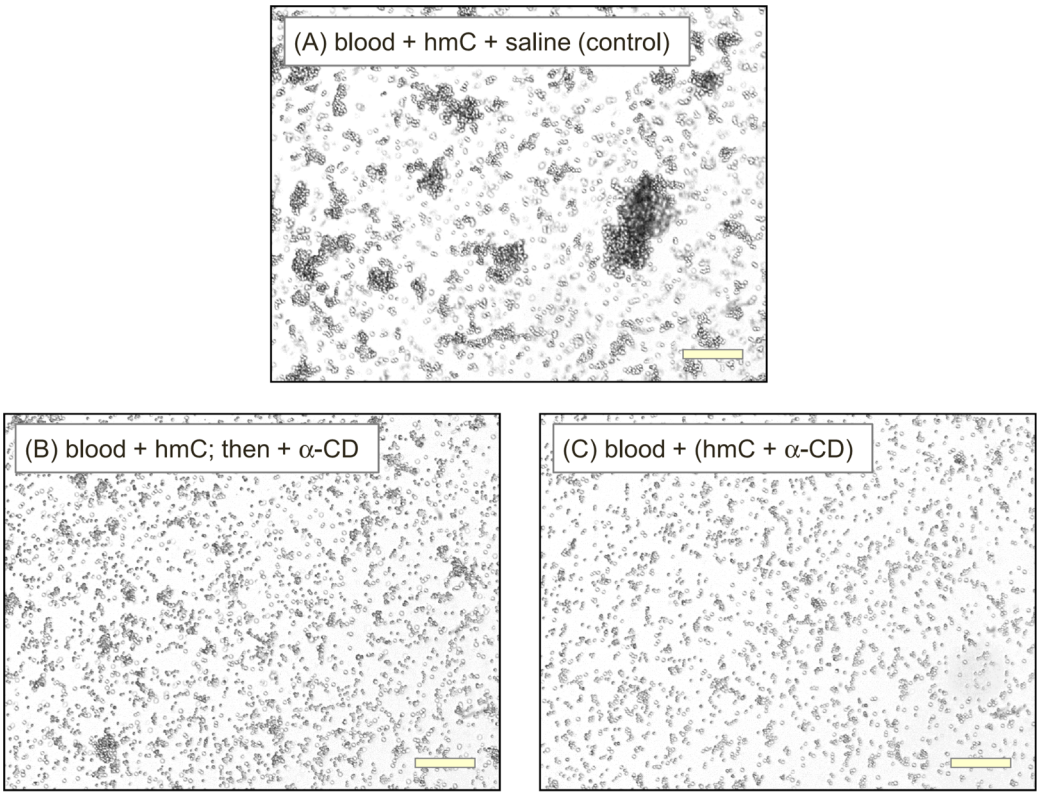

Figure 9. Effect of α-CD on the clustering of citrated bovine blood cells due to hmC. The hmC has 5 mol % of C_{12} hydrophobes. (A) Control case: blood is combined with hmC; then saline is added. (B) Blood is combined with hmC; afterward α-CD is added. (C) hmC is first combined with α-CD; then the mixture is combined with blood. In all three samples, the hmC concentration is the same (0.033 wt %), while in B and C, the α-CD concentration is the same (16.7 mM). Scale bars are 100 μm.

was premixed with the hmC and then added to blood. Both of these β-CDs reduce the clustering compared to that in the control (Figure 9A), but many clusters still do exist. The cluster areal fraction ($A_{cluster}$) in the case of mβ-CD is 11 ± 2%, and for hpβ-CD it is 20 ± 2%. Thus, neither of these β-CDs is as effective as α-CD in terms of reducing clustering.

DISCUSSION

From our studies, the following experimental findings have been established:

(1) *hmC induces clustering of blood cells*, whereas the parent chitosan does not.
(2) Clustering due to hmC *increases* with polymer MW and concentration, as well as with hydrophobe chain length and degree of hydrophobe modification.
(3) CDs, and in particular α-CD, *reduce or eliminate* the hmC-induced clustering of blood cells.

The clustering observed in microscopy experiments on hmC−blood mixtures *directly correlates* with the gelation seen in macroscopic studies with the same systems. Note that our microscopy studies have been done with diluted samples relative to those for which gelation has been reported previously.[9,10] In the latter, blood was at its original cellular concentration (here, it is diluted 10×), while hmC was added at 0.25 or 0.5 wt % (here it is 5× or 10× lower). Experimental confirmation of the link between clustering and gelation is also provided by Figure 1b. The vial contains 0.25% hmC (with 5 mol % of C_{12} hydrophobes) and undiluted blood; thus, it is a concentrated version of the sample in Figure 2A. From the photo, it is clear that the sample is a blood-gel that holds its weight in the vial. Rheological measurements confirm the gel-like nature of this sample (data identical to that reported previously;[9,10] not shown here). Moreover, adding α-CD to the vial in Figure 1b ungels the blood (it becomes free-flowing), as expected.[9,10] Thus, the *reversal of clustering* by the CDs in dilute hmC−blood mixtures, as per the microscopic images in Figure 9, also corresponds to the *reversal of gelation* in the macroscopic studies.

Having established a correlation between hmC-induced clustering of blood cells with gelation, a logical inference is that both must proceed by the *same mechanism*. In trying to decipher this mechanism, it is worth reflecting on the aspects that the micrographs in Figures 2−9 *do show* and also *do not show*. With this in mind, we first rule out a couple of alternative hypotheses for the mechansim before proceeding to what we believe is the right one.

Hypothesis 1. An initial hypothesis would be for the gel to arise by interconnections of hmC chains only, with the blood cells simply getting embedded in an hmC network. It is true that hmC, being an amphiphilic polymer, will tend to associate in water through its hydrophobes,[3,6] but interchain associations seem to be insignificant at the low hmC concentrations studied here (~0.05 wt %). The hmC solutions added to the blood in all of the studies presented here were free-flowing liquids of low viscosity, and they remained so even at 0.5 wt %.[6] Thus, we can rule out the case of hmC forming a gel on its own. Could the hmC chains connect into a network only when mixed with blood? If this unlikely scenario were to occur, we would expect to see individual blood cells trapped (non-diffusing) in a gel matrix. We would *not* expect to find clusters

https://dx.doi.org/10.1021/acs.langmuir.0c00409
Langmuir 2020, 36, 8357−8366

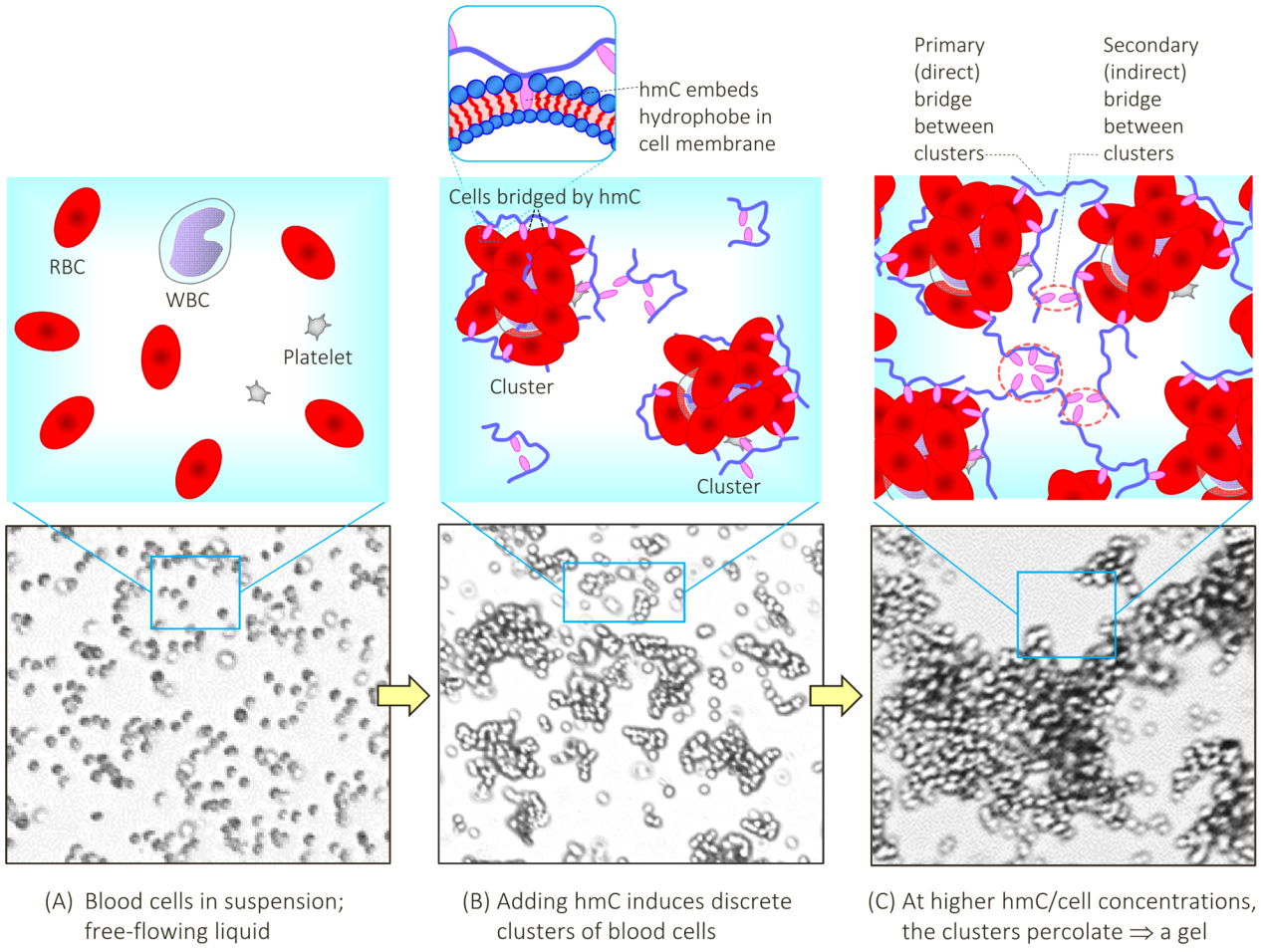

Figure 10. Mechanism by which hmC induces clustering and gelation of blood. Representative micrographs of blood cells are shown for three cases along with schematics of the postulated microstructure in each case. (A) Initially, blood is a low-viscosity liquid containing suspended cells, which include red blood cells (RBCs), white blood cells (WBCs), and platelets. (B) When hmC is added, the polymer chains induce the blood cells to aggregate into discrete clusters. This clustering is driven by the hydrophobic effect: hydrophobes (pink) attached to the hmC backbone (blue) embed into cell membranes, as highlighted by the inset at the top. The cell membrane is depicted as a bilayer of lipids with blue heads and red tails; the hydrophobic interior of the membrane has an affinity for the hydrophobes on hmC. When the same hmC chain binds to adjacent cells, it "bridges" the cells into clusters. (C) As the concentrations of cells and hmC are both increased, the clusters percolate through the sample volume, thus forming a network of clusters. Discrete clusters that are close to each other can be directly bridged by hmC chains; these are termed "primary" bridges. In addition, hmC chains that are bound to at least one cluster can interact with each other through their hydrophobes, leading to "secondary" bridges. The formation of a network transforms the liquid blood into a gel that has a significant yield stress.

of blood cells in the micrographs, which is what is actually observed.

Hypothesis 2. A second possibility is that the gel is formed by electrostatic interactions, either between polymer chains and blood cells or between polymer chains and proteins in the blood plasma. RBCs are known to have a negative surface (ζ) potential,[27] and the proteins in blood plasma are mostly anionic.[28] Chitosan and hmC, in contrast, are cationic, which makes them likely to interact electrostatically with blood components. However, in mixtures of blood with either chitosan (Figure 2A) or hmC of low hydrophobe content (0.5 mol %, Figure 5A and 1 mol %, Figure 5B), we see *no clustering of blood cells*. Even in concentrated mixtures of the above there is no gelation. These results are inconsistent with electrostatics being a key mechanism for gelation. Moreover, if interactions with blood plasma were an important factor, it would imply gelation *around* the blood cells, but again, we would not expect to find clusters of blood cells.

Hypothesis 3. The original hypothesis for the action of hmC on blood in our previous papers focused on *hydrophobic interactions*.[9,10] All of the studies in the current paper again point to hydrophobic interactions as the reason why hmC interacts with blood cells and moreover as the driving force for inducing clusters of these cells. Specifically, the key findings in this paper that can be explained only by hydrophobic interactions are that (a) clusters form only with hmC, not with chitosan, and (b) the more hydrophobes on hmC, the more clustering. On the basis of our results, we present a schematic depiction of hmC-induced effects on blood in Figure 10. Blood-cell clustering is shown in Figure 10B. Here, hmC chains are shown to bind to blood cells (see inset) by inserting their hydrophobic tails into cell membranes. When the same chain binds to adjacent blood cells, it *bridges the cells directly* and thereby induces clusters of the cells. Note that longer chains will be more conducive to bridging since the same chain can extend from one cell to another. This explains why more clustering is seen at the higher MW of hmC (Figure 8).

In considering the role of hydrophobic interactions, one key aspect is the affinity of hydrophobic tails for lipid bilayers. This affinity is known to increase exponentially with the length of

https://dx.doi.org/10.1021/acs.langmuir.0c00409
Langmuir 2020, 36, 8357−8366

the tails.[30,31] For example, it would be more than 10-fold higher for a C_{12} tail than for a C_8 tail. This aspect explains why there is significantly higher clustering of blood induced by an hmC with C_{12} hydrophobes (Figure 6D) than by an hmC with C_8 hydrophobes (Figure 6B). Also, the ability of CDs to reverse or eliminate the clustering is consistent only with hydrophobic interactions. Since CDs are nonionic, they cannot have any electrostatic effects in the system.[29] Thus, the likely way that CDs would undo the clusters is by competitively binding to the hydrophobes on hmC chains (i.e., the hydrophobes would then become sequestered in the binding pocket of the CDs).[8−10] Thereby, the connection of hmC to blood cells would be eliminated and so would the clusters.

Figure 10 also attempts to depict the progression from discrete clusters to networks (gels). In dilute mixtures of cells and hmC, which is the case for our microscopy studies, the clusters are discrete (Figure 10B). Conversely, in concentrated mixtures of the same, discrete clusters will aggregate and connect into a network that spans the entire sample volume (Figure 10C). Such a network will respond as a single unit and in an elastic fashion at low deformations, i.e., exhibit a gel-like response.[32,33] On the whole, we suggest that cluster−cluster aggregation (CCA) is the pathway from clusters to gels, i.e., it is clusters (not individual cells) that serve as the nodes of the network.[34−38] In our earlier mechanism from previous papers,[9,10] we had omitted such clusters and envisioned individual cells as the network nodes, but our new data from microscopy has made us revise our thinking on this point.

In the literature, there are models for diffusion-limited cluster−cluster aggregation (DL-CCA) and reaction-limited cluster−cluster cluster aggregation (RL-CCA).[34−38] Both of these models lead to network structures that are qualitatively similar to the above structure. The network in DL-CCA models tends to be more open and branched because the assumption is that the clusters will stick the moment they come into contact by diffusion.[34,36,37] In RL-CCA models, the network tends to be more dense because the clusters stick only after multiple contacts are made. We think the DL-CCA model is more likely to apply to blood−hmC mixtures. However, more work is needed to clarify this point.

One other element that is reflected in the schematic of the network in Figure 10C is the presence of hydrophobic associations between adjacent hmC chains that are also simultaneously interacting with blood cells. The lifetime of such hydrophobic associations will increase exponentially with hydrophobe length.[1,31] If the lifetime is sufficiently high, these associations could contribute additional cross-links to the network,[39,40] that is, cells would be bridged *indirectly* in this manner, and we refer to these as "*secondary*" bridges. The reason for invoking such indirect connections has to do with the geometry of the system. For gelation to occur in a blood−hmC mixture, the volume fraction of blood cells must be such that the cells nearly fill up the entire volume on their own. However, if the hmC induces dense clusters of some cells, the volume fraction could be reduced quite a bit. In such a scenario, the secondary bridges could still contribute to creation of a volume-filling network.

CONCLUSIONS

This study sought to obtain direct microscopic evidence as to how hmC converts a liquid suspension of blood cells into a gel. Working with dilute mixtures of hmC and blood, we found that hmC induces blood cells to aggregate into dense clusters. Such clusters are not formed in the case of the parent (unmodified) chitosan or if the hmC has too few hydrophobes. We established a systematic way to quantify the extent of clustering from the images. The extent of clustering increased with hydrophobic modification on the hmC as well as with the hydrophobe length ($C_{12} > C_{10} > C_8 > C_6$). These findings substantiate our original hypothesis that hydrophobic interactions drive the clustering. In other words, hmC chains insert their alkyl tails into the hydrophobic portions of cell membranes, and when hmC chains bind to adjacent cells, they bridge the cells into clusters. Further support for this hypothesis is provided by our finding that α-CD can reverse the hmC-induced clusters, which happens because α-CD molecules capture the hydrophobes in their binding pockets. Extrapolating from our current results, a macroscopic gel of hmC and blood arises at higher cell concentrations when the discrete clusters further aggregate and connect into a sample-spanning network of clusters. Hydrophobic associations between some adjacent hmC chains may also contribute to the connectivity of this network.

ASSOCIATED CONTENT

Supporting Information

The Supporting Information is available free of charge at https://pubs.acs.org/doi/10.1021/acs.langmuir.0c00409.

Details on the analysis of clustering; results for other cyclodextrins (PDF)

AUTHOR INFORMATION

Corresponding Authors

Matthew B. Dowling − *Department of Chemical & Biomolecular Engineering, University of Maryland, College Park, Maryland 20742, United States*; Email: mdowlin2@gmail.com

Srinivasa R. Raghavan − *Department of Chemical & Biomolecular Engineering, University of Maryland, College Park, Maryland 20742, United States*; orcid.org/0000-0003-0710-9845; Email: sraghava@umd.edu

Author

Ian C. MacIntire − *Department of Chemical & Biomolecular Engineering, University of Maryland, College Park, Maryland 20742, United States*

Complete contact information is available at: https://pubs.acs.org/10.1021/acs.langmuir.0c00409

Notes

The authors declare no competing financial interest.

ACKNOWLEDGMENTS

This work was supported by a grant from the NSF (DMR-1508155). We thank Dr. Brady Zarket, Dr. Vishal Javvaji, and Dr. Joseph White for helpful discussions.

REFERENCES

(1) Chassenieux, C.; Nicolai, T.; Benyahia, L. Rheology of associative polymer solutions. *Curr. Opin. Colloid Interface Sci.* **2011**, *16*, 18−26.

(2) de Molina, P. M.; Gradzielski, M. Gels obtained by colloidal self-assembly of amphiphilic molecules. *Gels* **2017**, *3*, 30.

(3) Desbrieres, J.; Martinez, C.; Rinaudo, M. Hydrophobic derivatives of chitosan: Characterization and rheological behaviour. *Int. J. Biol. Macromol.* **1996**, *19*, 21−28.

(4) Aranaz, I.; Harris, R.; Heras, A. Chitosan amphiphilic derivatives. Chemistry and applications. *Curr. Org. Chem.* **2010**, *14*, 308−330.
(5) Larsson, M.; Huang, W. C.; Hsiao, M. H.; Wang, Y. J.; Nyden, M.; Chiou, S. H.; Liu, D. M. Biomedical applications and colloidal properties of amphiphilically modified chitosan hybrids. *Prog. Polym. Sci.* **2013**, *38*, 1307−1328.
(6) Lee, J. H.; Gustin, J. P.; Chen, T. H.; Payne, G. F.; Raghavan, S. R. Vesicle-biopolymer gels: Networks of surfactant vesicles connected by associating biopolymers. *Langmuir* **2005**, *21*, 26−33.
(7) Lee, J. H.; Oh, H.; Baxa, U.; Raghavan, S. R.; Blumenthal, R. Biopolymer-connected liposome networks as injectable biomaterials capable of sustained local drug delivery. *Biomacromolecules* **2012**, *13*, 3388−3394.
(8) Chen, Y. J.; Javvaji, V.; MacIntire, I. C.; Raghavan, S. R. Gelation of vesicles and nanoparticles using water-soluble hydrophobically modified chitosan. *Langmuir* **2013**, *29*, 15302−15308.
(9) Dowling, M. B.; Kumar, R.; Keibler, M. A.; Hess, J. R.; Bochicchio, G. V.; Raghavan, S. R. A self-assembling hydrophobically modified chitosan capable of reversible hemostatic action. *Biomaterials* **2011**, *32*, 3351−3357.
(10) Javvaji, V.; Dowling, M. B.; Oh, H.; White, I. M.; Raghavan, S. R. Reversible gelation of cells using self-assembling hydrophobically-modified biopolymers: Towards self-assembly of tissue. *Biomater. Sci.* **2014**, *2*, 1016−1023.
(11) Tribet, C.; Vial, F. Flexible macromolecules attached to lipid bilayers: Impact on fluidity, curvature, permeability and stability of the membranes. *Soft Matter* **2008**, *4*, 68−81.
(12) Antunes, F. E.; Marques, E. F.; Miguel, M. G.; Lindman, B. Polymer-vesicle association. *Adv. Colloid Interface Sci.* **2009**, *147-48*, 18−35.
(13) Meister, A.; Blume, A. (Cryo)Transmission electron microscopy of phospholipid model membranes interacting with amphiphilic and polyphilic molecules. *Polymers* **2017**, *9*, 521.
(14) Meier, W.; Hotz, J.; GuntherAusborn, S. Vesicle and cell networks: Interconnecting cells by synthetic polymers. *Langmuir* **1996**, *12*, 5028−5032.
(15) Rao, Z.; Inoue, M.; Matsuda, M.; Taguchi, T. Quick self-healing and thermo-reversible liposome gel. *Colloids Surf., B* **2011**, *82*, 196−202.
(16) Ito, M.; Taguchi, T. Enhanced insulin secretion of physically crosslinked pancreatic beta-cells by using a poly(ethylene glycol) derivative with oleyl groups. *Acta Biomater.* **2009**, *5*, 2945−2952.
(17) Antunes, F. E.; Brito, R. O.; Marques, E. F.; Lindman, B.; Miguel, M. Mechanisms behind the faceting of catanionic vesicles by polycations: Chain crystallization and segregation. *J. Phys. Chem. B* **2007**, *111*, 116−123.
(18) Mizuta, R.; Taguchi, T. Hemostatic properties of in situ gels composed of hydrophobically modified biopolymers. *J. Biomater. Appl.* **2018**, *33*, 315−323.
(19) Vo, D. T.; Whiteley, C. G.; Lee, C. K. Hydrophobically modified chitosan-grafted magnetic nanoparticles for bacteria removal. *Ind. Eng. Chem. Res.* **2015**, *54*, 9270−9277.
(20) Vo, D. T.; Lee, C. K. Cells capture and antimicrobial effect of hydrophobically modified chitosan coating on Escherichia coli. *Carbohydr. Polym.* **2017**, *164*, 109−117.
(21) Chen, Z. H.; Yao, X. P.; Liu, L.; Guan, J.; Liu, M. Y.; Li, Z. H.; Yang, J.; Huang, S. J.; Wu, J. M.; Tian, F.; Jing, M. L. Blood coagulation evaluation of N-alkylated chitosan. *Carbohydr. Polym.* **2017**, *173*, 259−268.
(22) Huang, Y. C.; Zhang, Y.; Feng, L. B.; He, L. M.; Guo, R.; Xue, W. Synthesis of N-alkylated chitosan and its interactions with blood. *Artif. Cells, Nanomed., Biotechnol.* **2018**, *46*, 544−550.
(23) Behrens, A. M.; Sikorski, M. J.; Kofinas, P. Hemostatic strategies for traumatic and surgical bleeding. *J. Biomed. Mater. Res., Part A* **2014**, *102*, 4182−4194.
(24) De Castro, G. P.; Dowling, M. B.; Kilbourne, M.; Keledjian, K.; Driscoll, I. R.; Raghavan, S. R.; Hess, J. R.; Scalea, T. M.; Bochicchio, G. V. Determination of efficacy of novel modified chitosan sponge dressing in a lethal arterial injury model in swine. *J. Trauma* **2012**, *72*, 899−907.
(25) Dowling, M. B.; MacIntire, I. C.; White, J. C.; Narayan, M.; Duggan, M. J.; King, D. R.; Raghavan, S. R. Sprayable foams based on an amphiphilic biopolymer for control of hemorrhage without compression. *ACS Biomater. Sci. Eng.* **2015**, *1*, 440−447.
(26) Chaturvedi, A.; Dowling, M. B.; Gustin, J. P.; Scalea, T. M.; Raghavan, S. R.; Pasley, J. D.; Narayan, M. Hydrophobically modified chitosan gauze: a novel topical hemostat. *J. Surg. Res.* **2017**, *207*, 45−52.
(27) Diez-Silva, M.; Dao, M.; Han, J. Y.; Lim, C. T.; Suresh, S. Shape and biomechanical characteristics of human red blood cells in health and disease. *MRS Bull.* **2010**, *35*, 382−388.
(28) Alberts, B. *Molecular Biology of the Cell*; Garland Publishers, 2002.
(29) Szejtli, J. Introduction and general overview of cyclodextrin chemistry. *Chem. Rev.* **1998**, *98*, 1743−1753.
(30) Evans, D. F.; Wennerstrom, H. *The Colloidal Domain: Where Physics, Chemistry, Biology, and Technology Meet*; Wiley-VCH: New York, 2001.
(31) Israelachvili, J. N. *Intermolecular and Surface Forces*, 3rd ed.; Academic Press: San Diego, CA, 2011.
(32) Larson, R. G. *The Structure and Rheology of Complex Fluids*; Oxford University Press: Oxford, 1999.
(33) Graessley, W. W. *Polymeric Liquids & Networks: Dynamics and Rheology*; Taylor & Francis: New York, 2008.
(34) Meakin, P.; Jullien, R. The effects of restructuring on the geometry of clusters formed by diffusion-limited, ballistic, and reaction-limited cluster cluster aggregation. *J. Chem. Phys.* **1988**, *89*, 246−250.
(35) Lin, M. Y.; Lindsay, H. M.; Weitz, D. A.; Ball, R. C.; Klein, R.; Meakin, P. Universality in colloid aggregation. *Nature* **1989**, *339*, 360−362.
(36) Poon, W. C. K.; Haw, M. D. Mesoscopic structure formation in colloidal aggregation and gelation. *Adv. Colloid Interface Sci.* **1997**, *73*, 71−126.
(37) Lattuada, M.; Wu, H.; Morbidelli, M. A simple model for the structure of fractal aggregates. *J. Colloid Interface Sci.* **2003**, *268*, 106−120.
(38) Liu, P.; Heinson, W. R.; Sorensen, C. M.; Chakrabarty, R. K. Kinetics of sol-to-gel transition in irreversible particulate systems. *J. Colloid Interface Sci.* **2019**, *550*, 57−63.
(39) Biggs, S.; Habgood, M.; Jameson, G. J.; Yan, Y. D. Aggregate structures formed via a bridging flocculation mechanism. *Chem. Eng. J.* **2000**, *80*, 13−22.
(40) Swenson, J.; Smalley, M. V.; Hatharasinghe, H. L. M. Mechanism and strength of polymer bridging flocculation. *Phys. Rev. Lett.* **1998**, *81*, 5840−5843.

https://dx.doi.org/10.1021/acs.langmuir.0c00409
Langmuir 2020, 36, 8357−8366

Supporting Information for:

How Do Amphiphilic Biopolymers Gel Blood? An Investigation Using Optical Microscopy

Ian C. MacIntire, Matthew B. Dowling, and Srinivasa R. Raghavan*
Department of Chemical and Biomolecular Engineering, University of Maryland, College Park, MD 20742-2111
*Corresponding authors. Emails: sraghava@umd.edu, mdowlin2@gmail.com

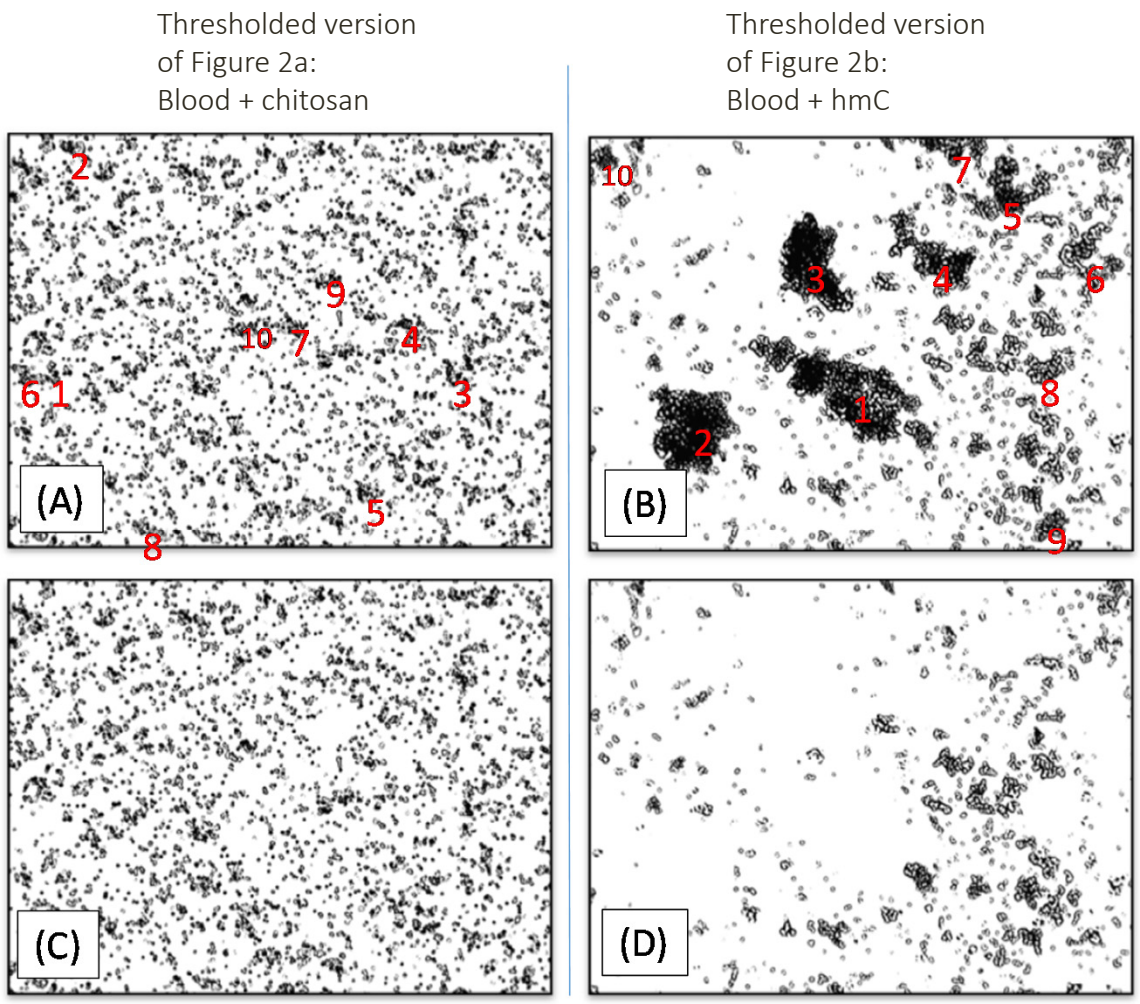

Figure S1. Quantifying the extent of clustering in optical micrographs. The images in Figure 2 showing the interaction of bovine blood cells with 0.05 wt% chitosan and hmC are analyzed using ImageJ. (A) and (B) are thresholded versions of Figures 2a and 2b, respectively. The 10 largest clusters in these images are identified with numbers (1 being the largest, then 2, and so on). (C) and (D) are the same images after removing these 10 largest clusters. Note that (C) seems nearly identical to (A), whereas (D) is very different from (B). That is, the 10 largest clusters occupy only ~ 5% of the total area in (A) whereas they occupy ~ 62% of the area in (B). Thus, the total area occupied by the 10 largest clusters can be used as a measure of the extent of clustering. The above procedure is repeated for 3 or more distinct images of the same sample (from different areas on the microscope grid). Thereby, the average and standard deviation for the normalized areal fraction are calculated.

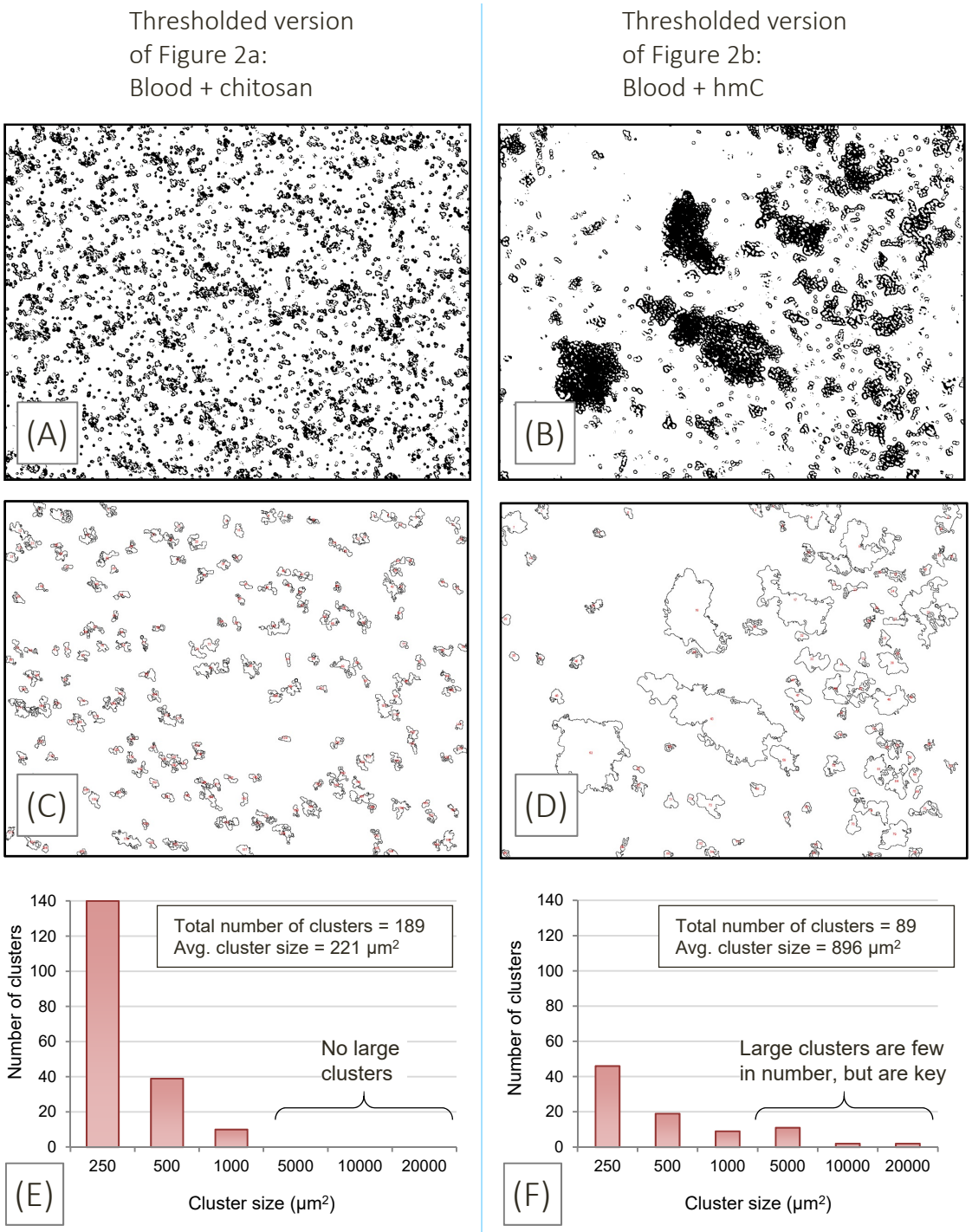

Figure S2. Why cluster size distributions are not useful in quantifying clustering in optical micrographs. (A) and (B) are thresholded versions of Figures 2a and 2b, identical to those in Figure S1. ImageJ is used to outline the clusters in these images, as shown in (C) and (D). Next, the cluster size distributions corresponding to (C) and (D) are plotted in (E) and (F). The size distribution is extremely skewed by the large clusters in the case of the hmC sample (F), which makes calculation of average cluster sizes unreliable. Conversely, for the chitosan sample (E), it is unclear if the small clusters are indeed clusters or if they are overlapping cells.

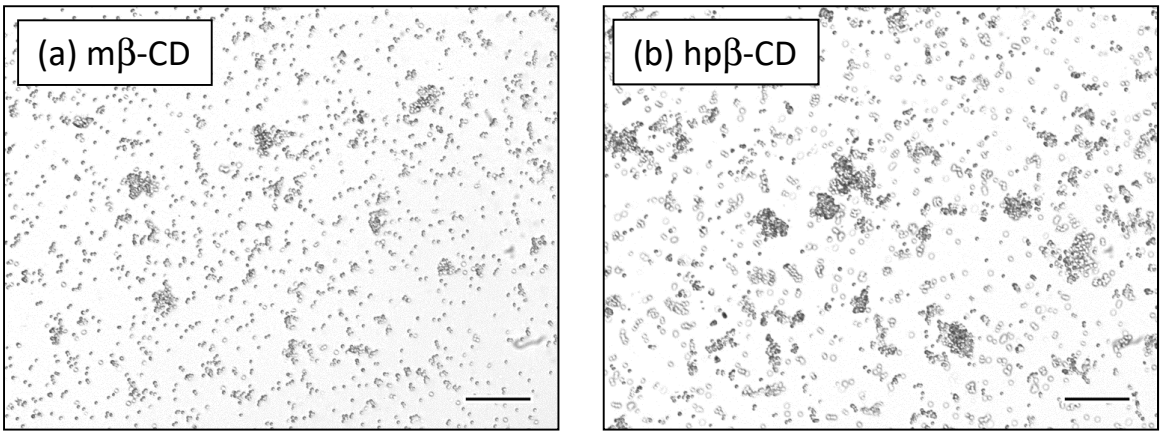

Figure S3. Effects of two β-CD derivatives on the clustering of citrated bovine blood cells due to hmC. The hmC has 5 mol% of C12 hydrophobes. The image in (a) is for mβ-CD and that in (b) for hpβ-CD. In these experiments, hmC was first combined with the CD, and then the mixture was combined with blood. The hmC concentration in the two samples is 0.033 wt% while the CD concentration in each case is 16.7 mM. Scale bars are 100 μm.